Intense X-ray induced formation of silver nanoparticles stabilized by biocompatible polymers

Article *in* Applied Physics A · November 2009

DOI: 10.1007/s00339-009-5377-x · Source: OAI

10 authors, including:

Changhai Wang
Max Planck Institute for Chemical Physics of Solids
41 PUBLICATIONS **1,030** CITATIONS
SEE PROFILE

Chia-Chi Chien
University of South Australia
46 PUBLICATIONS **891** CITATIONS
SEE PROFILE

Ru-Shi Liu
National Taiwan University
496 PUBLICATIONS **16,554** CITATIONS
SEE PROFILE

J. H. Je
Pohang University of Science and Technology
414 PUBLICATIONS **5,497** CITATIONS
SEE PROFILE

Appl Phys A (2009) 97: 295–300
DOI 10.1007/s00339-009-5377-x

Applied Physics A
Materials Science & Processing

Intense X-ray induced formation of silver nanoparticles stabilized by biocompatible polymers

Chang-Hai Wang · Chi-Jen Liu · Cheng-Liang Wang · Chia-Chi Chien · Y. Hwu · Ru-Shi Liu · Chung-Shi Yang · Jung-Ho Je · Hong-Ming Lin · G. Margaritondo

Received: 17 June 2009 / Accepted: 22 July 2009 / Published online: 20 August 2009

Abstract Colloidal Ag nanoparticles were formed by X-ray irradiation in the presence of a polymer. This new synthesis method is simple, rapid and leads to a high production yield. Compared to the citrate-reduced Ag colloidal, polymer-protected Ag nanoparticles are smaller in size and more stable—and therefore suitable for biomedical application—as verified by TEM observation, XAFS measurement and optical characterization. Ag nanoparticles so produced were also visualized in solution and in real time by a visible light microscope based on dark field light scattering. The color-derived size and distribution of Ag nanoparticles correlates well with the hydrodynamic size data.

PACS 81.16.Be · 81.07.Bc · 82.50.Kx · 78.67.Bf

C.-H. Wang · C.-J. Liu · C.-L. Wang · C.-C. Chien · Y. Hwu (✉)
Institute of Physics, Academia Sinica, Nankang, Taipei, Taiwan
e-mail: phhwu@sinica.edu.tw

C.-C. Chien · Y. Hwu
Department of Engineering and System Science, National Tsing Hua University, Hsinchu, Taiwan

Y. Hwu
Institute of Opto-Electronics Sciences, National Taiwan Ocean University, Keelung, Taiwan

R.-S. Liu
Department of Chemistry, National Taiwan University, Taipei, Taiwan

C.-S. Yang
Nanomedicine Research Center, National Health Research Institute, Zhunan, Taiwan

J.-H. Je
Department of Materials Science and Engineering, Pohang University of Science and Technology, Pohang, Korea

H.-M. Lin
Department of Materials Engineering, Tatung University, Taipei, Taiwan

G. Margaritondo
Ecole Polytechnique Fédérale de Lausanne (EPFL), 1015 Lausanne, Switzerland

1 Introduction

Metallic nanoparticles are playing an increasingly important role in nanoscience and nanotechnology [1–3]. Their physical, chemical and biomedical properties strongly depend on the composition, size, shape, surface characteristics and stability: this opens the door to effective control of such properties to match specific technological requirements.

The chemical reduction of metallic precursors by reducing agents provides a simple and reliable preparation method. However, its success relies on the addition of excess reductants that can result in contamination. To remove the remaining reaction by-products, purification procedures such as high-speed centrifugation are needed—making it difficult to maintain the morphology and dispersion of the colloidals. Furthermore, only large Ag nanoparticles (>10 nm) can be so produced and the nanosols tend to aggregate: surfactants are essential to control the size distribution and prevent aggregation. Unfortunately, typical surfactants are affected by biocompatibility problems that can jeopardize possible biomedical applications.

There has recently been considerable interest in irradiation-based methods to prepare metallic nanoparticles in solution [4–10]. Their most significant advantage is the absence of added reducing agents: such agents are automatically created by the interaction between the radiation and the

solution. In addition, polymer-stabilized metallic nanoparticles can be prepared with a one-pot process. Different kinds of radiation were used including ultraviolet and visible light [9–11], electron beams [12, 13], proton beams [14], gamma-rays [4, 5, 15–22] and X-rays [23–27].

We present here the successful test of a new method: stable silver nanoparticles with 5 nm size were prepared by directly exposing a bulk precursor solution to synchrotron X-rays. The colloidal stability, size distribution and biocompatibility of the particles were improved by including a polymer—polyethylene glycol (PEG) or polyvinyl pyrrolidone (PVP)—in the solution.

The advantages of this approach include: (1) a "clean" system without reducing agents or surfactants; (2) controllable particle size and surface properties with high colloidal stability; (3) rapid synthesis and high reduction yields thanks to the high X-ray flux.

2 Materials and methods

The X-ray source was a high brightness superconducting wavelength shifter (SWLS) at the BL01A beam line of the 1.5 GeV, 300 mA storage ring at NSRRC (National Synchrotron Radiation Research Center), Hsinchu, Taiwan [28, 29]. We used a "white" (unmonochromatized) beam with no optical elements except one set of beryllium and Kepton windows. A slit system produced a transversal beam section of 13×9 mm^2. The calculated X-ray photon flux absorbed by the precursor solutions was centered at ≈12.5 keV and ranged in photon energy from 6.5–30 keV [23–27]. The delivered dose rate absorbed by the precursor solution was 4.1 ± 0.6 kGy/sec as measured with a Fricke dosimeter (0.8N H_2SO_4) with an estimated G(Fe^+) value of 13.

All the chemicals were of reagent grade and used without additional purifications. All solutions were prepared using de-ionized water (18.2 MΩ cm, Millipore, Milli-Q®, MA, U.S.). The silver precursor was Silver Nitrate ($AgNO_3$, 0.1 N) from Acros Organics Inc., NJ, U.S. The concentration of precursor solution for X-ray exposure was 0.5, 1 or 2 mM.

To examine the effects of capping polymers and OH radical scavengers, PEG (MW 6000, Showa Inc., Japan), PVP (MW 10000, Tokyo Chemical Industry Co., Ltd., Japan) or isopropanol (Mallinckrodt Baker Inc., NJ, U.S.) were added to the precursor solution. Except when otherwise specified, for all exposures 10 ml of the precursor solution were placed in polypropylene conical tubes and transferred for X-ray irradiation. None of the solutions was deaerated before irradiation. The exposure time ranged from 30 sec to 3 min. In addition, citrate-reduced silver nanoparticles were also prepared following the procedures described in the literature [30, 31].

UV-VIS visible absorption spectra of the nanosols were measured using a JASCO spectrophotometer (Model V-570, JASCO Inc., Japan) with a 1 cm quartz cuvette. In some of the tests, the nanoparticle formation and morphology evolution were monitored during the exposure by a miniature UV-VIS spectrometer (Ocean Optics® USB4000, Ocean Optics Inc., U.S.) using a quartz cuvette as the container. The typical acquisition rate was 10 spectra/sec. The hydrodynamic size of the nanoparticles in solutions was measured by a dynamic light scattering (DLS) size analyzer (Horiba LB-500, Horiba co. Ltd, Japan). The particle morphology, structure and size were measured with a JEOL JEM 2010 F Field Emission Gun Transmission Electron Microscope (FEG-TEM) operating at 200 kV.

Samples for TEM measurements were prepared by placing droplets of nanoparticle-containing solution on carbon-coated Cu grids and allowing them to dry. The size of Ag nanoparticles was analyzed by counting over 100 individual particles in the TEM micrographs.

Near edge X-ray absorption fine structure (NEXAFS) spectroscopy provided information about the structure of nanostructured materials. The NEXAFS measurements were performed on the Ag L3 edge (3351 eV), at the 16A Beam Line of the National Synchrotron Radiation Research Center (NSRRC, Hsinchu, Taiwan). Powdered polymer-stabilized Ag nanoparticles were obtained by combining centrifugation and solvent evaporation under reduced pressure. The data were collected in the transmission mode at room temperature and under ambient atmosphere.

Dark field light scattering from Ag nanoparticles in solution was used to visualize the nanoparticles in their pristine state. We used an Olympus IX51 system adapted with CytoViva® (Aetos Technologies, Inc., Auburn, AL, USA) illumination and imaging system. The CytoViva system incorporated a fixed Koehler Illumination and a highly efficient hollow cone of light that made it possible to illuminate small objects, including nanoparticles [32].

This light scattering imaging technique is based on the intrinsic scattering properties of Ag nanoparticles and does not require staining or a contrast agent. A drop of Ag nanosol was added on the glass slide and sealed with a cover slip. Then objective oil (Olympus Inc.) was applied and the sample was transferred for the analysis.

3 Results and discussions

3.1 Formation of colloidal Ag

We previously succeeded in synthesizing Au nanoparticles by X-ray irradiation [23–27]. We thus initiated our Ag tests with a similar procedure. However, such tests—conducted

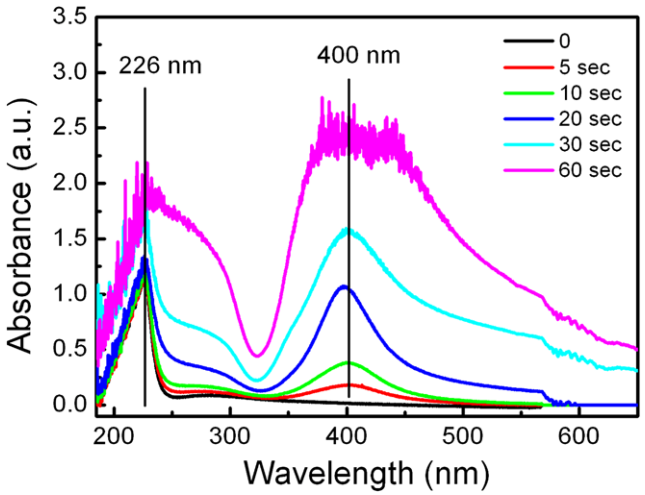

Fig. 1 Real-time UV-VIS absorption spectra of the precursor solution containing $AgNO_3$ and PEG during X-ray irradiation. Exposure time = 5–60 sec; $[AgNO_3] = 1$ mM; [PEG] = 0.3 mM. The volume of the precursor solution was 2 ml

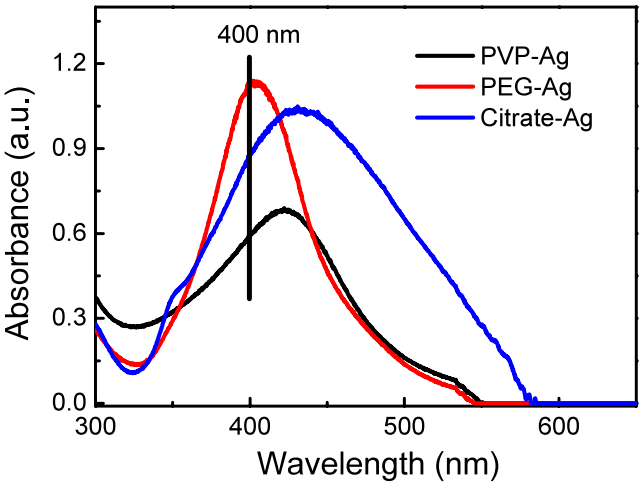

Fig. 2 UV-VIS absorption spectra of Ag nanoparticles (5× diluted to avoid saturation) prepared by X-ray irradiation in the presence of PEG or PVP or citrate reduction without polymers. For X-ray irradiation $[AgNO_3] = 0.5$ mM; irradiation time = 5 min; [PEG] = 0.3 mM; [PVP] = 0.12 mM. For citrate reduction: $[AgNO_3] = 0.833$ mM; [citrate] = 6.47 mM

with only $AgNO_3$ in the precursor solution—were not successful: no Ag particles were produced with up to 15 min X-ray irradiation. We can argue that Ag cannot be directly reduced by X-ray irradiation due to the redox potential difference of Au and Ag [33]. The addition of 2-propanol partially solved this problem, but the nanoparticle stability was not satisfactory. We therefore modified the strategy by adding PEG or PVP in different amounts to the precursor solution.

We monitored in real time the formation of colloidal Ag in the presence of a polymer by in situ UV-VIS optical absorption measurement. As illustrated in Fig. 1, the absorption maximum corresponding to the exposure time of 5 sec, 10 sec, 20 sec and 30 sec are 402.58 nm, 400.32 nm, 397.85 nm and 402.58 nm, respectively. These spectra show a blue shift up to 20 sec after which is followed by a pronounced red shift observed at 30 sec. The absorption signal saturated for 60 sec of exposure demonstrating a high conversion rate from silver ions to silver colloidal nanoparticles. Also note the absorption peak at 226 nm, which might be attributed to the transient silver clusters (e.g. Ag_4^{2+} as in [34, 35]), which are to be identified by further investigation.

The resulting Ag nanosols were stable for over one year in ambient environment. On the contrary, reference silver nanoparticle solutions prepared by citrate reduction (and no irradiation) tended to flocculate and precipitate. This is demonstrated in Fig. 2: the Ag SPR peak position is 404 nm, 422 nm or 432 nm and the full width at half maximum (FWHM) 83 nm, 113 nm or 149 nm for PEG-Ag, PVP-Ag and citrate-Ag. Compared to the PEG-Ag nanosols produced by X-ray irradiation, the absorption peak of the citrate-reduced Ag nanosol exhibits a large red shift of 28 nm and marked broadening, indicating indeed significant flocculation.

The Ag colloidal particles so produced are smaller in size than those of Au colloids [23–27] under similar experimental condition (specifically, precursor concentration and exposure time) and very stable. However, the synthesis of Ag nanosols has different features than that of Au. For example, pure gold nanosols can be synthesized since the addition of a polymer is not essential for Au; however, we found that $AgNO_3$ alone or $AgNO_3$ plus 2-propanol cannot produce stable Ag colloidals. In addition, the pH value of $AgNO_3$ cannot be adjusted to obtain a basic solution (flocculation occurs after adding NaOH) and a polymer such as PEG is essential for stable colloidal preparation.

3.2 Particle size measurements

Figures 3(a) and 3(c) show TEM results for Ag nanosols prepared in the presence of PEG for 5 sec and 5 min exposure; Figs. 3(b) and 3(d) show the corresponding size histograms. The measured particle size was 7.2 ± 2 nm for 5 sec exposure and the size distribution was broad. After 5 min exposure, the measured size was 5.2 ± 0.9 nm and the distribution was narrow. Equivalent results were obtained under similar experimental conditions for PVP-Ag (Fig. 3(e) to (h)): the measured size was 6.2 ± 2.9 nm and 3.8 ± 1.1 nm.

The hydrodynamic particle sizes for nanosols obtained with equivalent conditions to those of Fig. 3 in the presence of PEG or PVP ($[AgNO_3] = 1$ mM, [PEG] = 0.3 mM, [PVP] = 0.12 mM, exposure time = 5 min were 31.2 ± 10 nm and 25.6 ± 8 nm. Considering the TEM sizes, the thickness of the PEG and PVP coating layers was approximately 26 nm and 21 nm.

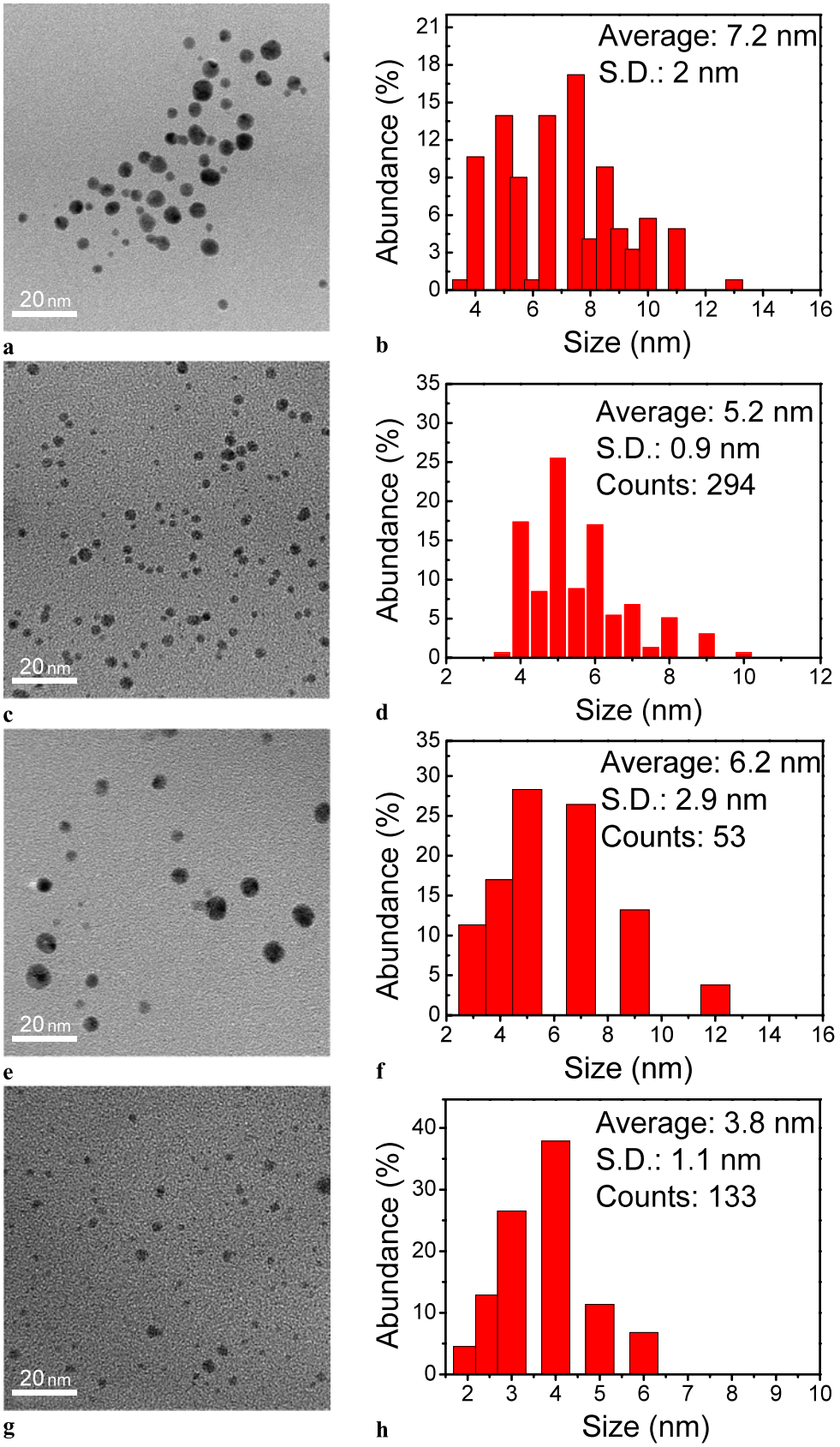

Fig. 3 Typical TEM micrographs and histograms showing the size and distribution of Ag nanoparticles with PEG and PVP stabilization. For all images and histograms, $[AgNO_3] = 1$ mM. (**a**) and (**b**): PEG added, [PEG] = 0.3 mM, 30 sec exposure; (**c**) and (**d**): [PEG] = 0.3 mM, 5 min exposure; (**e**) and (**f**): PVP added, [PVP] = 0.12 mM, 30 sec exposure; (**g**) and (**h**): [PVP] = 0.12 mM, 5 min exposure. Scale bar 20 nm

Note that the irradiation-induced morphological changes of PEG- or PVP-modified Ag colloidals are different from those for colloidal Au. With a short time irradiation, Au nanoparticles become interconnected and form network-like structures as we previously reported [23–27]. Such structures are not observed for Ag nanosols.

Ag L_3 NEXAFS spectra of Ag foil, $AgNO_3$ and PEG-Ag nanoparticles for different PEG concentrations are shown in Fig. 4. We observe a close similarity of the nanoparticle spectral features with those of Ag foil—whereas the $AgNO_3$ curve is very different. Note in particular the presence in the foil and nanoparticle curves of the absorption jump, shoulder and shape resonances. This indicates that our process yields complete or nearly complete reduction and a final atomic environment not very different from that of metallic Ag. Note, however, that the spectral features of the nanoparticle curves are substantially broader than those of metallic Ag.

3.3 Effect of 2-propanol as an OH radical scavenger

Strong oxidizing agents such as hydroxyl radicals are produced during the radiolysis of water [8, 15–17]. They can be expected to oxidize the previously formed Ag clusters to higher valence and therefore to prevent further production of colloidal Ag. Thus, we can expect a radical scavenger to counter this phenomenon.

Indeed, we found that OH radical scavenging by 2-propanol enhanced the colloidal Ag formation. However, the process yielded Ag particles that tended to flocculate and aggregate within a few days. These tests were performed both with and without polymers in the solution, and aggregation and flocculation was always present although not as marked in the presence of PVP.

The TEM micrograph of Fig. 5(a) (obtained 2-propanol and no polymer) illustrates the problem: the small particles formed a coagulate with each other and became big Ag bundles that continuously expanded until they eventually precipitated. As shown in Fig. 5(b), the presence of PEG did not eliminate this tendency to coagulation and precipitation. For PVP-Ag (Fig. 5(c)), this trend was also present although the nanosol appears to be relatively more stable. This phenomenon is not consistent with the results of laser [8, 15–17] or gamma-ray irradiation [15, 20–22]. Further investigations are underway to clarify this difference.

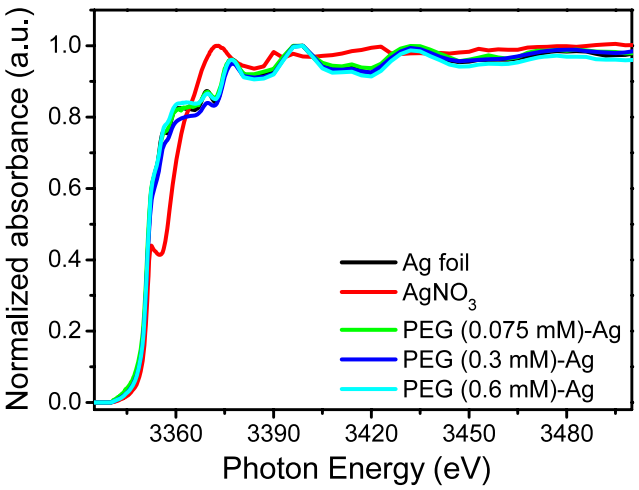

Fig. 4 NEXAFS spectra at Ag L_3 edge of Ag foil, $AgNO_3$ and PEG-Ag nanoparticles

3.4 Dark field light scattering imaging

Dark field imaging (CytoViva®) enabled us to visualize the nanoparticle motion in the solution in real time with no effect of the diffraction limit. Furthermore, the particle color is determined by the localized SPR peak position and can therefore be used to evaluate the particle size [36–38]. A representative dark field image of a PVP-Ag nanosol is shown in Fig. 6: individual Ag nanoparticle can be clearly identified. When analyzing the color distribution we found more blue particles (size 5–15 nm) than green particles (size 16–30 nm) and more green particles than red particles (size 31–46 nm) [38]. Thus, the size of most of the PVP-Ag nanoparticles is in the range of 10–30 nm, consistent with the hydrodynamic size measured by DLS. The particle size deduced by dark field reflects the overall dynamic size of the PEG-modified Ag nanoparticles in solutions. The larger size

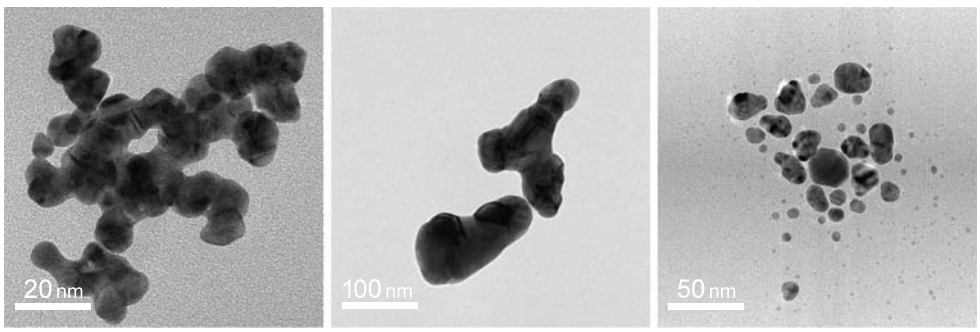

Fig. 5 TEM micrographs showing the effect of 2-propanol: (**a**) 1 mM [$AgNO_3$] + 2-propanol; (**b**) PEG-Ag + 2-propanol; (**c**) PVP-Ag + 2-propanol

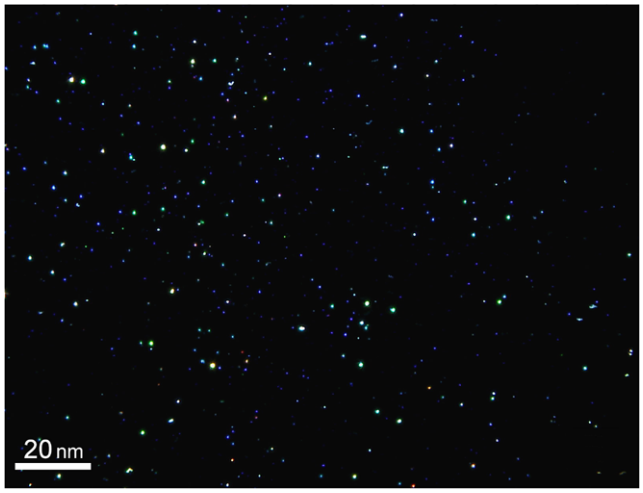

Fig. 6 Dark field light scattering image of PVP-Ag nanosols by an Olympus BX51 based Cytoviva microscope (100X oil objective). Scale bar = 20 μm

compared to the TEM-derived size is due to the immobilization of PEG "layer" on the Ag surfaces, which is consistent with the hydrodynamic size measured by DLS.

The marked Brownian motion of PEG-Ag nanoparticles in solution is illustrated in a video clip in the electronic supporting information. Even though particles bump into each other, coagulation and aggregation are seldom observed. In general, such results demonstrate that dark field imaging can be used for dynamic studies of nanoparticles in solution even in the presence of polymer stabilization.

4 Conclusions

We reported simple and effective method to prepare water-soluble Ag nanoparticles by X-ray irradiation in the presence of biocompatible PEG and PVP. This one-solution process produced very stable (lifetime exceeding 1 year) nanosols. The Ag nanoparticle size was 5–10 nm. The addition of an OH scavenger did not improve the process but led to nanosol instability. Overall, the process yields better biocompatibility, stability and size distribution than alternate methods and could be interesting in view of potential biomedical applications.

Acknowledgements This work was supported by the National Science Council, by the Academia Sinica (Taiwan), by the Creative Research Initiatives (Functional X-ray Imaging) of MOST/KOSEF (Korea), the Center for Biomedical Imaging (CIBM) in Lausanne, partially funded by the Leenaards and Jeantet foundations, by the Swiss National Fonds de la Recherche Scientifique and by the EPFL.

References

1. S.R. Nicewarner-Pena, Science **294**, 137 (2001)
2. L.A. Dick, A.D. Mafarland, C.L. Haynes, R.P. Van Duyne, J. Phys. Chem. B **106**, 7729 (2002)
3. M. Ferrari, Nat. Rev. Cancer **5**, 16 (2005)
4. Y.J. Zhu, Y.T. Qian, X.J. Li, M.W. Zhang, Chem. Commun. **5**, 1081 (1997)
5. Y.D. Yin, X.L. Xu, C.J. Xia, X. W Ge, Z.C. Zhang, Chem. Commun. **6**, 941 (1998)
6. Y.H. Chen, C.S. Yeh, Chem. Commun. **9**, 371 (2001)
7. J.P. Abid, H.H. Girault, P.F. Brevet, Chem. Commun. **9**, 829 (2001)
8. J.P. Abid, A.W. Wark, P.F. Brevet, H.H. Girault, Chem. Commun. **10**, 792 (2002)
9. H.H. Huang, X.P. Ni, G.L. Loy, C.H. Chew, K.L. Tan, F.C. Loh, J.F. Deng, G.Q. Xu, Langmuir **12**, 909 (1996)
10. V. Amendola, M. Meneghetti, J. Mater. Chem. **17**, 4705 (2007)
11. J.P. Abid, A.W. Wark, P.F. Brevet, H.H. Girault, Chem. Commun. **10**, 792 (2002)
12. S. Inasawa, M. Sugiyama, S. Koda, Jpn. J. Appl. Phys. **42**, 6705 (2003)
13. B.F.G. Johnson, K.M. Sanderson, D.S. Shephard, D. Ozkaya, W.Z. Zhou, H. Ahmed, M.D.R. Thmas, L. Gladden, M. Mantle, Chem. Commun. **8**, 1317 (2000)
14. S.K. Mahapatra, K.A. Bogle, S.D. Dhole, V.N. Bhoraskar, Nanotechnology **18**, 135602 (2007)
15. K. Wu, X.L. Xu, X.W. Ge, Z.C. Zhang, Radiat. Phys. Chem. **50**, 585 (1997)
16. Belloni, M. Mostafavi, H. Remita, J.-L. Marignier, M.-O. Delcourt, New J. Chem., 1239 (1998)
17. Gachard, H. Remita, J. Khatouri, B. Keita, L. Nadjo, J. Belloni, New J. Chem., 1257 (1998)
18. A. Henglein, D. Meisel, Langmuir **14**, 7392 (1998)
19. A. Henglein, Langmuir **15**, 6738 (1999)
20. M.K. Temgire, S.S. Joshi, Radiat. Phys. Chem. **71**, 1039 (2004)
21. B. Soroushian, I. Lampre, J. Belloni, M. Mostafavi, Radiat. Phys. Chem. **72**, 111 (2005)
22. T.H. Li, H.G. Park, S.H. Choi, Mater. Chem. Phys. **105**, 325 (2007)
23. K. Ferdi, E. Gulay, O. Eda, S. Sefik, Langmuir **21**, 437 (2005)
24. Y.C. Yang, C.H. Wang, Y.K. Hwu, J.H. Je, Mater. Chem. Phys. **100**, 72 (2006)
25. C.C. Kim, C.H. Wang, Y.C. Yang, Y.K. Hwu, S.K. Seol, Y.B. Kwon, C.H. Chen, H.W. Liou, H.M. Lin, G. Margaritondo, J.H. Je, Mater. Chem. Phys. **100**, 292 (1996)
26. C.H. Wang, T.E. Hua, C.C. Chien, Y.L. Yu, T.Y. Yang, C.J. Liu, W.H. Leng, Y. Hwu, Y.C. Yang, C.C. Kim, J.H. Je, C.H. Chen, H.M. Lin, G. Margaritondo, Mater. Chem. Phys. **106**, 323 (2007)
27. C.H. Wang, C.C. Chien, Y.L. Yu, C.J. Liu, C.F. Lee, C.H. Chen, Y. Hwu, C.S. Yang, J.H. Je, G. Margaritondo, J. Synchrotron Radiat. **14**, 477 (2007)
28. S. Baik, H.S. Kim, M.H. Jeong, C.S. Lee, J.H. Je, Y. Hwu, G. Margaritondo, Rev. Sci. Instrum. **75**, 4355 (2004)
29. G. Margaritondo, Y. Hwu, J.H. Je, Riv. Nuovo Cimento Ser. 4 **27**(7), 1–40 (2004)
30. J. Turkevich, P.C. Stevenson, J. Hiller, Discuss. Faraday Soc. **11**, 55 (1951)
31. Z.S. Pillai, P.V. Kamat, J. Phys. Chem. B **108**, 945–951 (2004)
32. T.A. Hasling, Microsc. Today **14**, 22–26 (2006) –26
33. C.H. Hamann, A. Hamnett, W. Vielstich, *Electrochemistry* (Wiley-VCH Verlag GmbH, Weinheim, 1998)
34. T. Linnert, P. Mulvaney, A. Henglein, H. Weller, J. Am. Chem. Soc. **112**, 4657 (1990)
35. C. Petit, P. Lixon, M.P. Pileni, J. Phys. Chem. **97**, 12974 (1993)
36. C.F. Bohren, D.R. Huffman, *Absorption and Scattering of Light by Small Particles* (Wiley, New York, 1993), pp. 287–380
37. U. Kreibig, M. Vollme, *Optical Properties of Metal Clusters* (Springer, Berlin, 1995), pp. 14–123
38. K.J. Lee, P.D. Nallathamby, L.M. Browning, C.J. Osgood, X.H.N. Xu, ACS Nano **1**, 133–143 (2007)